Developmental Biology **223,** 17–26 (2000)
doi:10.1006/dbio.2000.9734, available online at http://www.idealibrary.com on IDEAL®

Real-Time Measurements of the Interactions between Fluorescent Speract and Its Sperm Receptor

Takuya Nishigaki[1] and Alberto Darszon

Departamento de Genética y Fisiología Molecular, Instituto de Biotecnología, Universidad Nacional Autónoma de México, Cuernavaca, Morelos 62250, México

Lytechinus pictus **sea urchin sperm express receptors for speract, a sperm-activating peptide derived from the homologous egg jelly coat. We found that the fluorescence of fluorophore-labeled, active, speract analogs is quenched upon receptor binding. This property allowed us to perform real-time measurements of speract–receptor interactions using intact sperm and to determine, for the first time, their association (k_{on}) and dissociation (k_{off}) rate constants. The high k_{on} (2.4×10^7 M^{-1} s^{-1}) and low k_{off} (4.4×10^{-6} s^{-1} (95%) and 3.7×10^{-4} s^{-1} (5%)) can account for the sperm response to picomolar concentrations of speract. We also examined the influence of extracellular ions on speract–receptor interactions using the fluorescence quenching method described in this study. The association rate of speract to the receptor is dramatically reduced in Na^+-free seawater (NaFSW), divalent cation-free seawater (DCFSW), and high-K^+ seawater (HKSW). In seawater speract induces an increase in intracellular pH (pHi), while it is unable to do so in either NaFSW or HKSW. To test if the lack of this pHi change causes the reduction in the speract association rate, pHi was increased with NH_4Cl (10 mM) at the time labeled speract was added. Interestingly, this procedure completely (in HKSW) or partially (in NaFSW and DCFSW) restored the speract association rate to its receptor. These findings indicate that an increase in sperm pHi positively affects the receptor binding activity for this peptide and may partially explain the positive binding cooperativity displayed by the speract receptor.**

Key Words: **fertilization; sperm-activating peptide; receptor; fluorescence quenching; real-time measurement.**

INTRODUCTION

Sperm-activating peptides (SAPs)[2] (Suzuki, 1995) are diffusible components of the echinoderm egg jelly coat. They are among the best characterized molecules involved in gamete interaction. It has been proposed that the physiological function of SAPs is to attract sperm to the egg (Ward *et al.*, 1985), accelerate sperm penetration through the jelly coat (Suzuki and Garbers, 1984), and promote the acrosome reaction (Yamaguchi *et al.*, 1987; Nishigaki *et al.*, 1996).

Speract (or SAP-1), Gly-Phe-Asp-Leu-Asn-Gly-Gly-Gly-Val-Gly, was the first purified and structurally identified SAP (Suzuki *et al.*, 1981; Garbers *et al.*, 1982). Thereafter, this peptide has been used as a model to study the physiological function of SAPs and the underlying signal transduction pathways. Speract is thought to bind to its receptor (Smith and Garbers, 1983; Dangott and Garbers, 1984; Shimizu *et al.*, 1994) on the plasma membrane of sperm flagella (Cardullo *et al.*, 1994) and transiently activate guanylate cyclase (Bentley *et al.*, 1986). The increased cGMP levels activate a K^+-selective ion channel (Cook and Babcock, 1993; Galindo *et al.*, 2000) which hyperpolarizes the sperm membrane potential (Babcock *et al.*, 1992). This hyperpolarization may activate several voltage-dependent membrane proteins such as a Na^+/H^+ exchange system (Lee and Garbers, 1986), adenylate cyclase (Beltrán *et al.*, 1996), and a poorly selective K^+ channel (Labarca *et al.*, 1996; Gauss *et al.*, 1998), which contribute to intracellular alkalinization, elevation of intracellular concentration of cAMP,

[1] To whom correspondence should be addressed. Fax: (52-73) 172388. E-mail: takuya@ibt.unam.mx.

[2] Abbreviations used: $[Ca^{2+}]i$, intracellular Ca^{2+} concentration; DCFSW, divalent cation-free seawater; $DiSC_3(5)$, 3,3′-dipropylthiadicarbocyanine iodide; Em, membrane potential; F-speract, 5(6)-SFX-labeled speract; GC, guanylate cyclase; HKSW, high-K^+ seawater; k_{on}, association rate constant; k_{off}, dissociation rate constant; LC7SW, low-Ca^{2+} pH 7.0 seawater; NaFSW, Na^+-free seawater; pHi, intracellular pH; R-speract, 5(6)-TAMRA-X-labeled speract; SAP, sperm-activating peptide; 5(6)-SFX, 6-(fluorescein-5-(and 6-)carboxamido)-hexanoic acid, succinimidyl ester; 5(6)-TAMRA-X, SE, 6-(tetramethylrhodamine-5-(and 6-)carboxamido)hexanoic acid, succinimidyl ester.

0012-1606/00 $35.00

and membrane depolarization, respectively. In addition, intracellular Ca^{2+} concentration ($[Ca^{2+}]i$) transiently increases by activation of a Ca^{2+} channel and/or a Na^+/Ca^{2+} exchanger (Schackmann and Chock, 1986). Speract is also known to induce dephosphorylation of membrane-bound guanylate cyclase and lipid hydrolysis and oxidation (reviewed in Darszon *et al.*, 1999).

Although the speract receptor has been extensively studied (Smith and Garbers, 1983; Dangott and Garbers, 1984; Shimizu *et al.*, 1994; Cardullo *et al.*, 1994), the kinetics of its interaction with speract have not been described in detail. Here, we performed real-time binding experiments in whole sperm utilizing fluorescence quenching of fluorophore-labeled, active speract and obtained association and dissociation rate constants for the speract–receptor interactions for the first time. Furthermore, we examined the effects of ionic composition of seawater and pHi on the speract–receptor association kinetics and demonstrated that the speract receptor is very sensitive to the chemical milieu. The physiological consequences of the properties of the speract receptor revealed in this study are discussed.

MATERIALS AND METHODS

Materials. *Lytechinus pictus* sperm were obtained by intracoelomic injection of 0.5 M KCl and "dry sperm" were kept on ice. Artificial seawater (ASW) consisted of (mM) 486 NaCl, 10 $CaCl_2$, 10 KCl, 27 $MgCl_2$, 29 $MgSO_4$, 2.5 $NaHCO_3$, 0.1 EDTA, and 10 Hepes (pH 8.0 with NaOH). Na^+-free seawater (NaFSW) consisted of (mM) 486 choline chloride, 10 $CaCl_2$, 7.5 KCl, 27 $MgCl_2$, 29 $MgSO_4$, 2.5 $KHCO_3$, and 10 Hepes (pH 8.0 with *N*-methyl-D-glucamine). Divalent cation-free seawater (DCFSW) was as ASW but without Ca^{2+} and Mg^{2+} salts. Low-Ca^{2+} pH 7.0 seawater (LC7SW) was as ASW but with 1 mM $CaCl_2$ and at pH 7.0 and was used for preincubation of sperm for all experiments. In the binding experiments, 0.1% BSA was added to the seawater to avoid nonspecific binding of ligand. Fluorophores 6-(fluorescein-5-(and 6-)carboxamido)hexanoic acid, succinimidyl ester (5(6)-SFX) and 6-(tetramethylrhodamine-5-(and 6-)carboxamido)hexanoic acid, succinimidyl ester (5(6)-TAMRA-X, SE) were from Molecular Probes. Speract was from Peninsula Laboratories, Inc.

Sperm Em, pHi, and $[Ca^{2+}]i$ measurements. Changes in sperm membrane potential, pHi, and $[Ca^{2+}]i$ induced by speract were determined as previously described (Gonzáles-Martínes *et al.*, 1992), using $DiSC_3(5)$, dimethylcarboxyfluorescein, and Quin-2, respectively. Em responses to speract and F-speract in *Strongylocentrotus purpuratus* sperm were performed in hypotonic seawater (1/10 diluted ASW with distilled water), since swollen sperm undergo larger speract-induced membrane potential changes (Babcock *et al.*, 1992).

Labeling speract with fluorophores. Speract (5–10 nmol) was dissolved in 100 μl of 200 mM sodium borate buffer, pH 8.5, containing about fivefold labeling-reagent, 5(6)-SFX or 5(6)-TAMRA-X. The solution was stirred well and incubated for 1 h at room temperature. The excess reagents were blocked by adding 10 μl of 1 M glycine to the solution and incubated for 30 min at room temperature. Labeled peptides were purified by reverse-phase HPLC, and their concentrations were determined by amino acid analysis.

Fluorescence measurements. Fluorescence intensity and spectra were recorded on an Aminco SLM 8000 spectrofluorimeter. Sample solution (1.5–2 ml) was measured in a glass tube at 15°C. Real-time binding experiments were performed under gentle magnetic stirring. For centrifugation binding experiments, free and bound ligands were separated by centrifugation at maximum velocity (16,000*g*) in a microfuge for 1 min, and the fluorescence intensity of the supernatant (free ligand concentration) was determined.

Data processing. Incomplete fluorescence quenching of F-speract was corrected by using the following equation: $F_{corrected} = F_c - (F_c - F)/0.88$, where F is the fluorescence intensity of F-speract with sperm and F_c is the fluorescence intensity of F-speract without sperm. The association rate constant (k_{on}) was obtained by using the following equation: $k_{on} = v_0/([L_0] \times [R_0])$, where v_0, $[L_0]$, and $[R_0]$ indicate the initial velocity of ligand association, total ligand concentration, and total receptor concentration, respectively. Total receptor concentrations were determined by the fluorescence quenching methods described in Fig. 5a. Dissociation rates (B/B_0) were obtained by using the following equation: $B/B_0 = (F_c - F)/(F_{c0} - F_0)$, where F_0 and F_{c0} indicate the values of F and F_c at $t = 0$.

RESULTS

Properties of fluorophore-labeled speract analogs upon binding to the receptor. Speract receptors were shown to be localized on *S. purpuratus* sperm flagella by using the fluorescent speract analog, FITC-GGG[Y^2]-speract (Cardullo *et al.*, 1994). Attempts to reproduce this result using 5(6)-SFX-labeled speract (F-speract) failed despite the fact that F-speract induced the same membrane potential changes in *S. purpuratus* sperm as unlabeled speract (Fig. 1a). This result could indicate that fluorescence quenching was occurring upon ligand–receptor binding.

This possibility was explored by measuring emission spectra of F-speract in the absence or presence of sperm. Due to seasonal availability, *L. pictus* sperm were used in all experiments presented hereafter. Speract induces changes in Em, pHi, and $[Ca^{2+}]i$ in similar fashions in *L. pictus* and *S. purpuratus* sperm (Fig. 1b). As shown in Fig. 2a, the emission peak of F-speract remarkably decreased in the presence of sperm. When an excess of unlabeled speract was added to the F-speract solution in the presence of sperm, emission of F-speract was almost the same as that in the absence of sperm. When 5(6)-TAMRA-X-labeled speract (R-speract) was used, its fluorescence also decreased upon binding to the receptor (Fig. 2b). These results indicate that the fluorescence of the fluorophores is quenched when ligand–receptor complexes are formed and explain the difficulty of detecting sperm-bound labeled speract by fluorescence microscopy.

Thereafter, competition experiments were performed to quantitatively assess the binding activity of fluorophore-labeled speract analogs to the receptor. When R-speract (1 nM) was used as a ligand, both unlabeled speract and F-speract almost equally competed with R-speract for receptor binding (Fig. 3a). This result indicates that F-speract is a useful tool to study ligand–receptor interactions. Similar

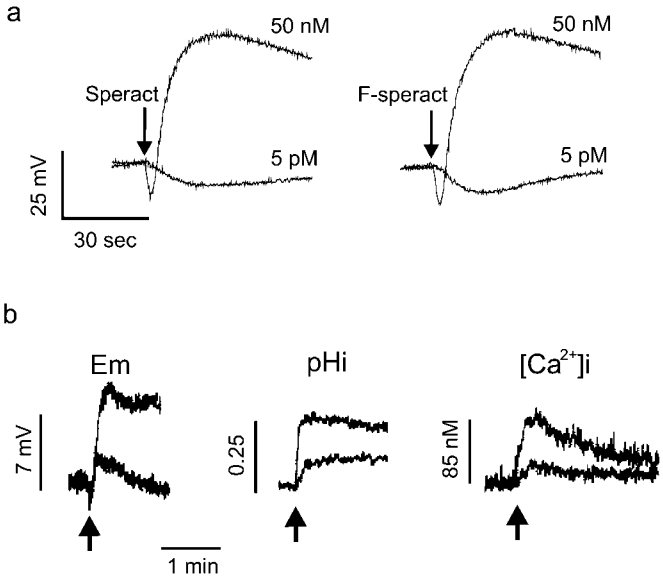

FIG. 1. Sperm response to speract. (a) Speract and F-speract induce similar membrane potential (Em) changes in *S. purpuratus* sperm. Sperm (10 μl of 1/10 diluted dry sperm) were suspended in 2 ml of hypotonic seawater (1/10 diluted ASW) containing 0.5 μM $DiSC_3(5)$, and fluorescence was monitored at 620 nm excitation and 670 nm emission every 0.2 s (5 Hz). Oligomycin (0.5 μM) was added to the sperm suspension to eliminate mitochondrial Em before adding speract or F-speract. Em responses to 5 pM and 50 nM of speract (left) and F-speract (right) are shown. A downward deflection indicates hyperpolarization, an upward deflection depolarization. (b) Speract responses in *L. pictus* sperm. Speract-induced changes in sperm Em, pHi, and $[Ca^{2+}]i$ were measured as previously described (Gonzáles-Martínes *et al.*, 1992), using $DiSC_3(5)$, dimethylcarboxyfluorescein, and Quin-2, respectively. Arrows indicate the time when speract was added to sperm (10–25 μl of 1/10 diluted dry sperm) suspended in 0.8 ml of ASW. The upper traces represent responses to 100 nM speract, the lower ones to 5 pM speract. Representative traces from at least five independent experiments are shown.

experiments were performed to assess the binding activity of R-speract using F-speract as a ligand. In contrast to F-speract, R-speract competed with the ligand more effectively than unlabeled speract (Fig. 3b), suggesting that R-speract has higher affinity for the receptor than unlabeled speract. Therefore, we used mainly F-speract to explore the interactions between speract and its receptor. Centrifugation binding experiments at various sperm concentrations in the presence and absence of unlabeled speract indicated that nonspecific binding of F-speract is not significant in the sperm concentration range used in this study (Fig. 3c).

To determine if the quenching of F-speract when it binds to the receptor can be used to quantitatively describe the characteristics of the speract–receptor interactions, the results obtained by the fluorescence quenching method were compared with those derived from a centrifugation method. First, the labeled ligand (1 nM F-speract) was incubated with various concentrations of sperm, and the free ligand concentration was measured by the two methods (Fig. 4a). Next, competition curves were obtained by adding increasing concentrations of unlabeled speract to the ligand solution containing a fixed concentration of sperm using the

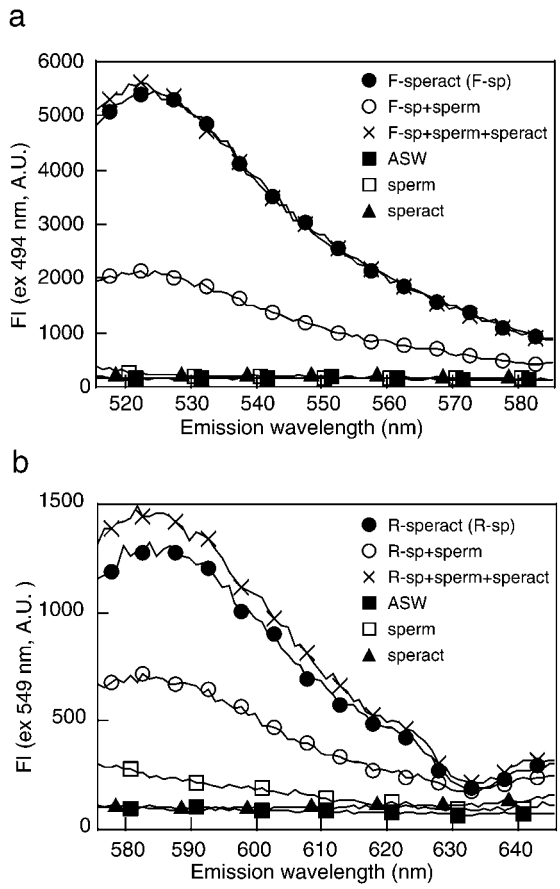

FIG. 2. Emission spectra of labeled speract analogs. (a) F-speract. Samples were excited at 494 nm, and emission spectra were scanned from 515 to 585 nm. In all figure legends FI is the fluorescence intensity and A.U. is an arbitrary fluorescence unit. This figure shows 1 nM F-speract (closed circle), 1 nM F-speract with sperm (open circle), 1 nM F-speract with sperm in the presence of 1 μM unlabeled speract (X), ASW only (closed rectangle), sperm (open rectangle), and 1 μM speract (closed triangle). The scan was initiated after 10 min incubation of the ligand and sperm. In the cases of ASW, sperm, and speract symbols are displayed for every 10 points of data. For the other conditions symbols for every 5 data points are shown. (b) R-speract. Samples were excited at 549 nm and emission spectra were obtained from 575 to 646 nm. This figure shows 1 nM R-speract (closed circle), 1 nM R-speract with sperm (open circle), 1 nM R-speract with sperm in the presence of 1 μM unlabeled speract (X), ASW only (closed rectangle), sperm (open rectangle), and 1 μM speract (closed triangle). Samples were processed as in the case of F-speract but R-speract was used instead. The results are the averages of three measurements, having SD smaller than the symbols. Similar results were obtained in at least two other experiments.

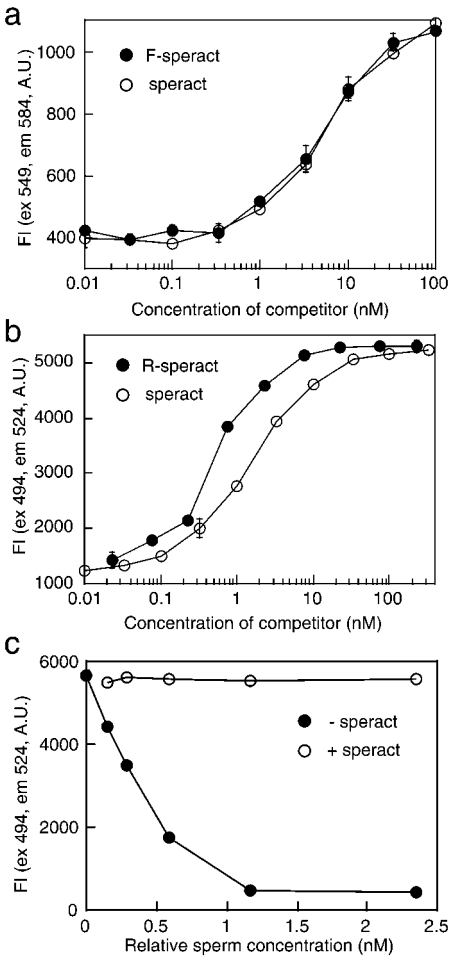

FIG. 3. Properties of fluorophore-labeled speract analogs. (a) Competition activity of F-speract for the receptor. R-speract (1 nM) used as ligand was mixed with various concentrations of F-speract (closed circle) or unlabeled speract (open circle) to compete for receptor binding. The fluorescence of R-speract was measured after 30 min incubation of the ligand with spermatozoa. The net R-speract emission was obtained by subtracting the background fluorescence of F-speract. (b) Competition activity of R-speract for the receptor. F-speract (1 nM) was used as ligand, and R-speract (closed circle) and unlabeled speract (open circle) were utilized as competitors. The net F-speract emission was obtained by subtracting the background fluorescence of R-speract. (c) Assessment of nonspecific binding. F-speract (1 nM) was incubated with various concentrations of sperm in the presence (open circle) or absence (closed circle) of unlabeled speract (1 μM). After 1 h incubation the samples were centrifuged and the fluorescence intensity of the supernatant was measured. Relative sperm concentration indicates the total speract receptor concentration measured as described for Fig. 5a. All data are the means of three measurements. Error bars (±SD) are displayed only when they are larger than the symbols. Similar results were obtained in at least two other experiments.

two methods (Fig. 4b). These experiments showed that the fluorescence of F-speract was not quenched 100% upon receptor binding. We estimated the percentage of quenching to be 88% from the above data. When the result derived from the quenching method is corrected considering the incomplete quenching, it gives results that are consistent with the centrifugation method (insets of Fig. 4). Thus, the

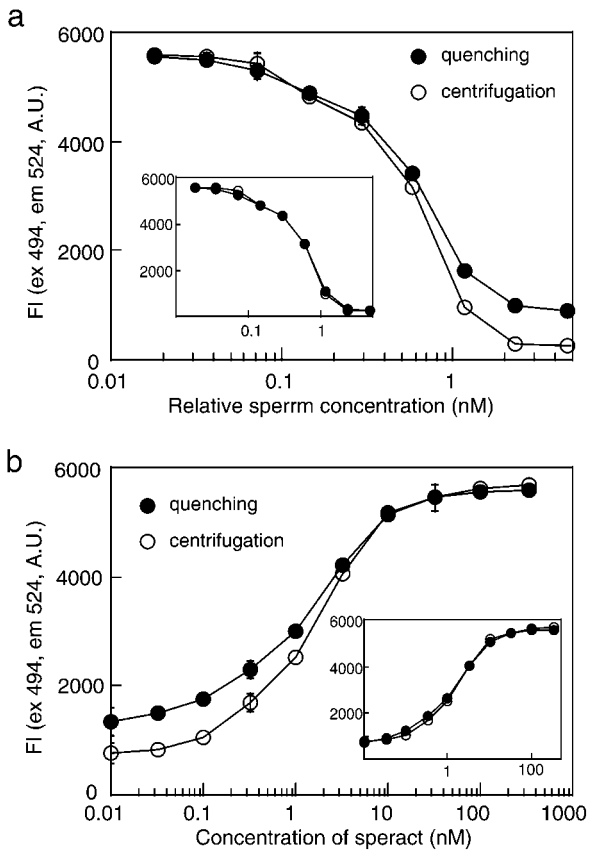

FIG. 4. The quenching ratio of F-speract upon receptor binding. (a) Binding experiments using fluorescence quenching and centrifugation. F-speract (1 nM) was incubated in a glass tube (2 ml) with various concentrations of sperm for 60 min at 15°C, and then fluorescence intensities of the suspensions were measured (closed circle). Immediately after that the suspensions were centrifuged and fluorescence intensities of the supernatant (free F-speract) were determined (open circle). Data shown in the quenching method were corrected by subtraction of sperm intrinsic fluorescence. Sperm concentrations were expressed as in Fig. 3c. (b) Competition binding experiments measured by the two methods. F-speract (1 nM) was mixed with various concentrations of unlabeled speract and incubated with sperm (1 nM speract receptor) for 60 min at 15°C. Thereafter the fluorescence intensities of the suspensions (closed circle) and the supernatant after centrifugation (open circle) were measured. Sperm intrinsic fluorescence was subtracted for the quenching method. The insets (both a and b) show results of the quenching method after correction for incomplete quenching (88%) as described under Materials and Methods. All data represent the means of three measurements. Error bars (±SD) are displayed only when they are larger than the symbols. Similar results were obtained in at least two other experiments.

quenching method can be used in quantitative studies of receptor binding.

Real-time measurement of the kinetics of the ligand–receptor interactions in normal ASW. First, we measured the total concentration of speract receptor using the fluorescence quenching method. When the free ligand concentration is more than 100 times higher than the K_d for its receptor, most receptors (>99%) will be occupied with the ligand (Hulme *et al.*, 1992). Thus, we incubated sperm containing around 1 nM speract receptor (1000- to 5000-fold dilution of "dry sperm") with 10 nM F-speract and measured the decrease in fluorescence intensity (Fig. 5a), assuming that the K_d of speract for its receptor is smaller than 0.1 nM, which was demonstrated to be true in this study. This rapid and easy determination of the total receptor concentration was carried out prior to all binding experiments to perform them under appropriate conditions. Counting the number of cells in the sperm suspension with a hemacytometer after fixing sperm with glutaraldehyde, the maximal speract binding sites (B_{max}) on a single sperm cell were determined to be $6.3 \pm 0.53 \times 10^4$ sites/cell ($n = 5$).

Next, association kinetics of the ligand–receptor interaction were measured by the fluorescence quenching method using lower concentrations of F-speract (0.5 or 1.0 nM) to determine the association rate constant (k_{on}) of the speract receptor. Figure 5b shows representative speract binding kinetics to the receptor. Background fluorescences of ASW and sperm were subtracted and incomplete quenching was corrected in the figure. The k_{on} was determined to be $2.4 \pm 0.21 \times 10^7$ M^{-1} s^{-1} ($n = 5$) using the concentration of F-speract and receptor and initial velocity of the ligand association as described under Materials and Methods.

Thereafter, the dissociation rate constant (k_{off}) of the speract receptor was studied using the fluorescence quenching method. Ligand dissociation was initiated by adding an excess of unlabeled speract 30 min after F-speract binding had been started. Figure 6a shows that F-speract dissociated very slowly; however, it dissociated rapidly when cells were solubilized with Triton X-100. This fast dissociation was observed even when the detergent was added in the absence of unlabeled speract (data not shown), indicating that the speract receptor rapidly loses its affinity for speract upon detergent solubilization (Bentley *et al.*, 1988).

Dissociation kinetics were then measured, keeping the samples in the dark to avoid bleaching of fluorescence of F-speract (see Fig. 6a inset) and exposing them to light only to measure the fluorescence intensity. The results show that F-speract dissociation is extremely slow and biphasic with a minor fast component contributing 5% of the total binding (3.7×10^{-4} s^{-1}) and a major (resting 95%) slower component (4.4×10^{-6} s^{-1}) as seen in Figs. 6b and 6c.

Ionic composition of ASW influences speract–receptor interactions. Smith and Garbers (1983) demonstrated that speract–receptor interactions are very sensitive to the ionic environment in equilibrium binding experiments. We further explored this aspect by measuring association kinetics of F-speract to the receptor by the quenching method. When

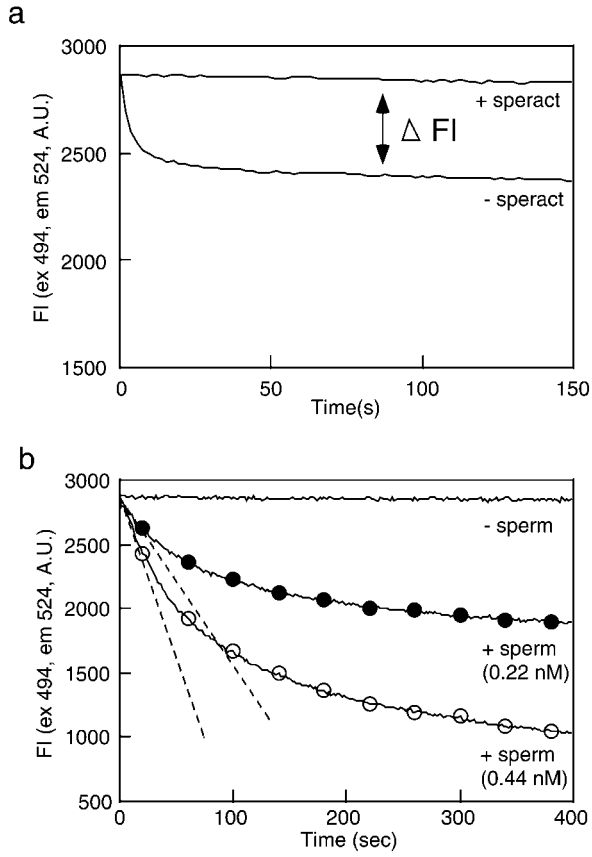

FIG. 5. Real-time measurement of F-speract association to the receptor in normal ASW. (a) Measurement of total receptor concentration. Sperm preincubated in LC7SW was added to a glass tube containing 10 nM F-speract in normal ASW at $t = 0$ in the presence (upper line) or absence (lower line) of 4 μM unlabeled speract. Fluorescence intensity was measured every 2 s. Total receptor concentration was calculated from the reduction of fluorescence intensity, about 8 min after addition of sperm, considering the quenching ratio of 88%. (b) F-speract association kinetics to the receptor. Experiments were performed as above, except for using a lower concentration of F-speract (0.5 nM). Data were corrected as in the insets of Fig. 4. The samples are without sperm (line only) and with sperm containing 0.22 nM receptor (closed circle) or 0.44 nM receptor (open circle). Slopes indicated by broken lines express initial velocities of the ligand association to the receptor. Symbols are displayed every 20 data points. All data are the averages of three measurements, having SD smaller than the symbols. One representative experiment of five is shown.

Na^+ was substituted by choline (NaFSW), F-speract did not bind any more to the receptor, as expected (Fig. 7a). Addition of 0.5% normal seawater to NaFSW (about 2.5 mM Na^+ final concentration) was enough to obtain 50% of the receptor binding activity. F-speract was also unable to bind to its receptor in DCFSW (Fig. 7b). Adding 10% normal seawater to DCFSW (about 5 mM Mg^{2+} and 1 mM Ca^{2+} final) was enough to obtain 50% of the normal receptor

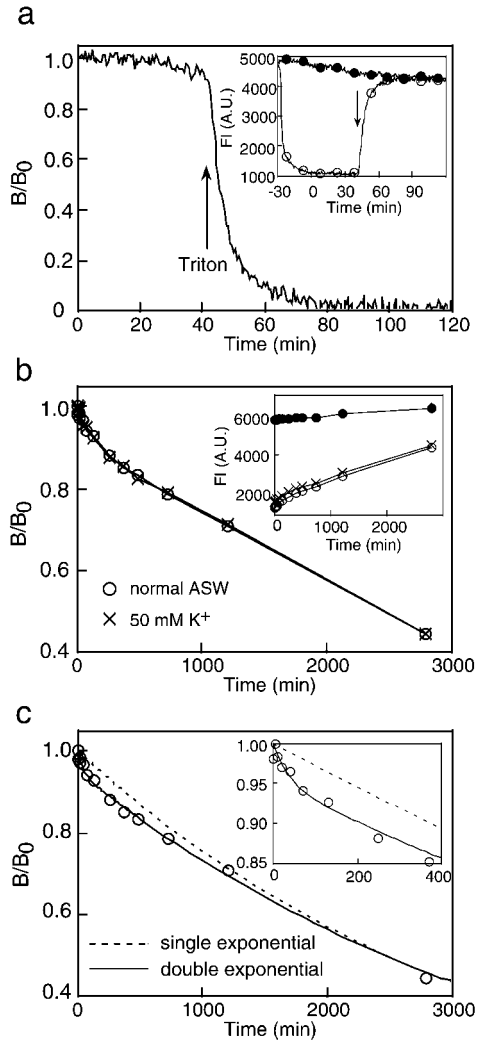

FIG. 6. Dissociation kinetics of F-speract from the receptor. (a) Continuous monitoring of F-speract dissociation. Sperm (0.9 nM speract receptor) were incubated with 1 nM F-speract for 30 min and ligand dissociation was initiated at $t = 0$ by adding 1 μM unlabeled speract to the suspension. Triton X-100 (0.05% final) was added to the suspension at $t = 40$ (arrow). Just before adding Triton X-100, DNase I (0.05 mg/ml final) was added to avoid an increase in viscosity. The fluorescence intensity of the sample with (open circle) and without sperm (closed circle) is shown in the inset. The sample was continuously exposed to excitation light (ex 494 nm, em 524 nm). Fluorescence values were measured every 30 s. Symbols in the inset are displayed every 30 points. Dissociation rates (B/B_0) were obtained as described under Materials and Methods. One representative experiment of four is shown. (b) Slow ligand dissociation. Experiments were carried out similarly with sperm (0.7 nM speract receptor) except that continuous exposure of the ligand (1 nM F-speract) to the excitation light was avoided. Fluorescence intensity was measured at the times indicated, otherwise the samples were kept in the dark without stirring. The samples are without sperm (closed circle, inset), with sperm in normal ASW (open circle), and with sperm in 50 mM K^+ ASW (X). Each point is the mean of three measurements, having SD smaller than the symbols. Similar results were obtained in at least two other experiments. (c) Comparison of experimental and theoretical data for the dissociation kinetics. The broken line represents a single exponential function using $k_{off} = 4.7 \times 10^{-6}$ s^{-1}. To fit the experimental results (open circles, normal ASW) a double exponential function was used considering two k_{off}, 3.7×10^{-4} s^{-1} (5%) and 4.4×10^{-6} s^{-1} (95%). The fitting was done using SigmaPlot ($R^2 = 0.996$). The inset has an expanded time axis.

binding activity. Added individually, Mg^{2+} appeared slightly more potent than Ca^{2+} (Fig. 7c). Though K^+-free seawater did not affect the kinetics of F-speract binding, high-K^+ seawater (HKSW) decreased the ligand association rate (Fig. 7d). This alteration is most probably caused by the decrease in the association rate constant because the dissociation rate constant did not change in HKSW (Fig. 6b).

It is well known that speract cannot elevate sperm pHi in HKSW or NaFSW as it does in normal ASW (Lee and Garbers, 1986). Thus, we examined how a pHi increase influences the speract association kinetics by adding 10 mM NH_4Cl to HKSW. Interestingly, addition of NH_4Cl completely reversed the inhibition effect of high K^+ (Fig. 8a). Furthermore, positive effects of NH_4Cl on speract–receptor interactions were observed in NaFSW and DCFSW (Figs. 8b and 8c), although the ligand–receptor interactions did not completely recover under the latter conditions. In contrast, NH_4Cl had a very small effect in normal ASW (Fig. 8d).

Our results indicate that conditions that prevent speract from increasing sperm pHi remarkably reduce its association rate to the receptor and this reduction is restored by alkalinization of pHi with NH_4Cl. Therefore, sperm pHi is an important factor that regulates the ligand binding activity of the speract receptor.

DISCUSSION

We found that the 5(6)-SFX- and 5(6)-TAMRA-X-labeled speract analogs (F- and R-speract) are active and their fluorescence is quenched upon receptor binding. Using F-speract, which has almost the same affinity for the receptor as unlabeled speract (Fig. 3a), incomplete quenching upon receptor binding (12%) could be corrected after estimating free fluorescent ligand by centrifugation (Fig. 4). Thus, fluorescence quenching of F-speract allowed us to perform quantitative real-time measurements of speract–receptor interactions conveniently under conditions under which artifacts of sperm autofluorescence and turbidity are negligible. This is to our knowledge one of a few successful reports of real-time measurements of ligand–receptor interactions using intact cells. The fact that echinoderm sperm have an extraordinary amount ($0.6–11 \times 10^4$ binding sites/cell) of high-affinity receptors for sperm-activating peptide (Smith and Garbers 1983; Shimizu *et al.*, 1994; Yoshino and

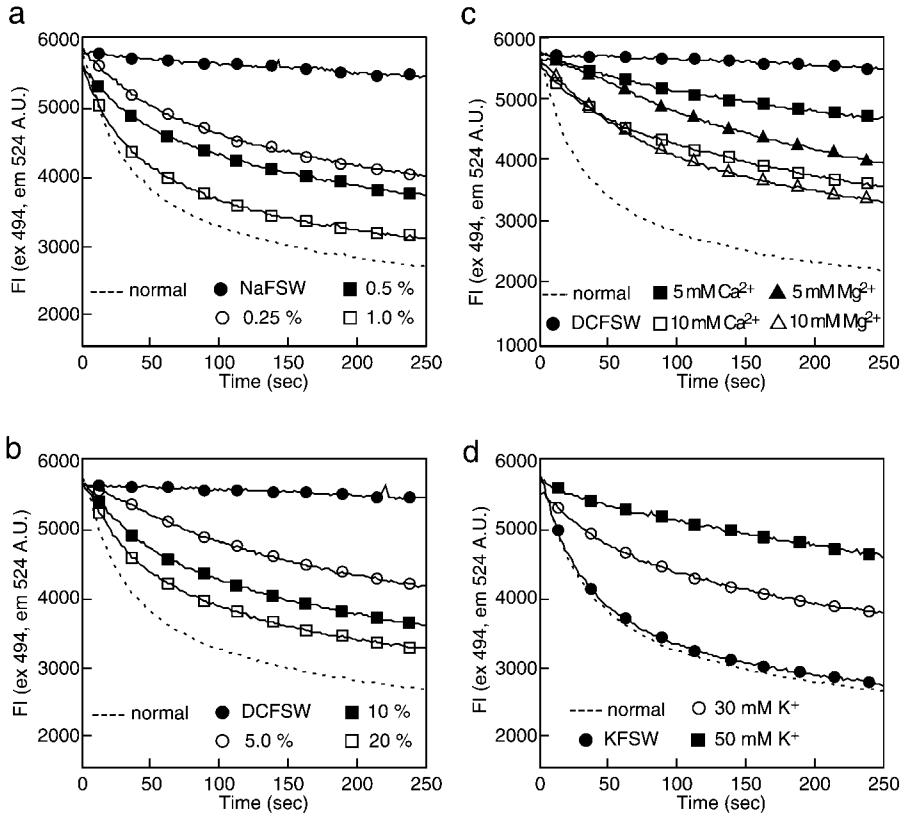

FIG. 7. The ion composition of ASW modulates F-speract association kinetics to the receptor. F-speract (1 nM) binding kinetics to the receptor (0.7 nM for a, b, and d, 0.8 nM for c) was measured as described for Fig. 5b. Fluorescence intensities are shown without correction for the incomplete quenching. (a) Effect of Na^+. NaFSW was mixed with normal ASW to prepare ASW containing various concentrations of Na^+. The samples are normal ASW (broken line), NaFSW (closed circle), 0.25% normal ASW (open circle), 0.5% normal ASW (about 2.5 mM Na^+, closed rectangle), and 1% normal ASW (open rectangle). (b) Effect of divalent cations. DCFSW was mixed with normal ASW to prepare ASW containing various concentrations of divalent cations. The samples are normal ASW (broken line), DCFSW (closed circle), 5% normal ASW (open circle), 10% normal ASW (about 1 mM Ca^{2+} and 5 mM Mg^{2+}, closed rectangle), and 20% normal ASW (open rectangle). (c) Individual effects of Ca^{2+} and Mg^{2+}. The samples are normal ASW (broken line), DCFSW (closed circle), 5 mM Ca^{2+} (closed rectangle), 5 mM Mg^{2+} (closed triangle), 10 mM Ca^{2+} (open rectangle), and 10 mM Mg^{2+} (open triangle). (d) Effect of K^+. The samples are normal ASW (10 mM K^+, broken line), K^+ free (closed circle), 30 mM K^+ (open circle), and 50 mM K^+ (closed rectangle). Symbols are displayed every 10 points for all data. Each point is the average of three measurements, having SD smaller than the symbols. The results from this experiment were reproduced at least four times.

Suzuki, 1992; Nishigaki *et al.*, 2000) permits this experimental approach.

Using this fluorescence quenching method, the maximal speract binding sites (B_{max}) in *L. pictus* sperm were calculated to be 6.3×10^4/cell (Fig. 5a). This number is nine times larger than that reported for *S. purpuratus* (Smith and Garbers, 1983), but similar for *Hemicentrotus pulcherrimus* (Shimizu *et al.*, 1994). Next, we determined both association and dissociation rate constants for the speract–receptor interactions. The k_{on} determined from the initial association velocity is high (2.4×10^7 M^{-1} s^{-1}); in contrast the k_{off} is extremely low and biphasic (3.7×10^{-4} s^{-1} (5%), 4.4×10^{-6} s^{-1} (95%)). This slow dissociation is probably not due to receptor internalization because similar results were obtained when ligand dissociation was initiated after short incubation time (5 min) of the ligand and the receptor (data not shown). In *S. purpuratus*, less than 20% of radiolabeled speract dissociated from the receptor after 60 min (Dangott and Garbers, 1984). Thus, the slow dissociation of speract from the receptor seems a common property of the speract receptor regardless of the species. The two distinct k_{off} values suggest that two different receptor types or two different states of a receptor exist. However, it was not possible to estimate two apparent k_{on} values from our data. According to the conventional calculation ($K_d = k_{off}/k_{on}$), two K_d values were estimated using one k_{on} value: 15 (5%) and 0.19 pM (95%). Considering that picomolar concentrations of speract have significant effects on sperm (Fig. 1), the K_d values estimated in this study are physiologically more reasonable than those estimated (nM range) in other species

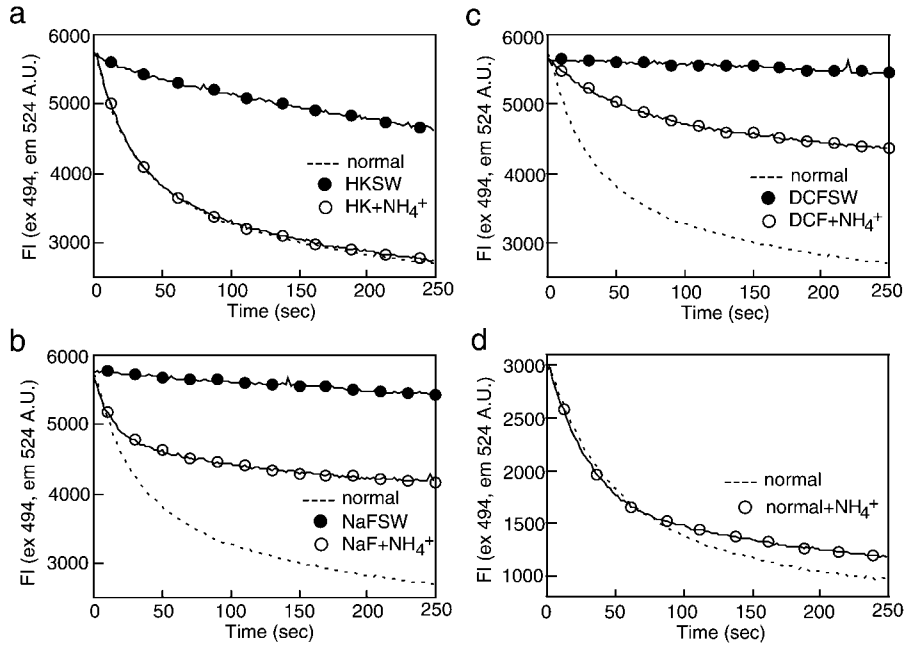

FIG. 8. NH_4Cl reverses the inhibition of F-speract association to its receptor in high-K^+, Na^+-free, and divalent cation-free SW. F-speract (1 nM) binding kinetics to the receptor (0.7 nM) were measured as for Fig. 5b. Fluorescence intensities are shown without correction for the incomplete quenching. (a) High-K^+ SW. The samples are normal ASW (broken line), 50 mM K^+ SW (closed circle), and 50 mM K^+ SW with 10 mM NH_4Cl (open circle). (b) Na^+-free SW. The samples are normal ASW (broken line), NaFSW (closed circle), and NaFSW with 10 mM NH_4Cl (open circle). (c) Divalent cation-free SW. The samples are normal ASW (broken line), DCFSW (closed circle), and DCFSW with 10 mM NH_4Cl (open circle). (d) Effect of NH_4Cl in normal ASW. In this experiment 0.5 nM F-speract was used in normal ASW (broken line) and with 10 mM NH_4Cl (open circle). Symbols are displayed every 10 points for all data. Each point is the average of three measurements, having SD smaller than the symbols. The results from this experiment were reproduced at least four times.

by using a radioactive speract analog in equilibrium binding experiments (Smith and Garbers, 1983; Shimizu *et al.*, 1994). These latter values possibly reflect an overestimation of the free ligand concentration and/or conditions of incomplete binding equilibrium.

Regulation of speract receptor. Our kinetic studies show that Na^+ is physiologically essential for the speract–receptor interactions, as demonstrated in equilibrium binding experiments by Smith and Garbers (1983). In addition, we found that the association rate of speract to the receptor decreases in HKSW (Fig. 7d). This result was surprising since under this condition the speract–receptor interactions were not affected in equilibrium binding experiments (Harumi *et al.*, 1992). Speract increases sperm pHi in normal ASW while it does not in either HKSW or NaFSW (Lee and Garbers, 1986). Interestingly, addition of NH_4^+, which increases pHi (Roos and Boron, 1981), to HKSW completely restored the ligand association kinetics (Fig. 8a). Moreover, NH_4^+ also accelerated ligand association in NaFSW (Fig. 8b). These findings suggest that pHi regulates the binding activity for the speract receptor.

In addition, Smith and Garbers (1983) reported that Mg^{2+}, but not Ca^{2+}, is important for speract association to the receptor. Since divalent cations influence SAP–receptor interactions in starfish, *Asterias amurensis* (Nishigaki *et al.*, 2000), this matter was further explored. Both Ca^{2+} and Mg^{2+} affect speract–receptor interactions, although Mg^{2+} seems more important than Ca^{2+} (Fig. 7c). Other divalent cations (Mn^{2+}, Sr^{2+}, and Co^{2+}) also accelerated the ligand association in DCFSW (data not shown), indicating that divalent cations have a positive effect on speract–receptor interactions in general. Addition of NH_4^+ to DCFSW also restored the speract association rate to the receptor, although partially (Fig. 8c). This result suggests that external divalent cations may participate in sperm pHi regulation. Further studies are necessary to clarify the relation between sperm pHi and external divalent cations.

In normal ASW (pH 8.0), NH_4^+ had only a minor effect on the speract–receptor interactions in sperm (Fig. 8d). This is not surprising since speract itself increases sperm pHi in normal seawater. If the k_{on} of the speract receptor at rest was smaller than that at high pHi, the receptor would be positively regulated by a speract-induced alkalinization. Positive binding cooperativity has been reported for the speract receptor and other SAP receptors using equilibrium binding (Shimizu *et al.*, 1994; Yoshino and Suzuki, 1992). This phenomenon may be partially explained by the effect of pHi on the receptor.

Guanylate cyclase (GC) is thought to be associated with the speract receptor in *S. purpuratus* (Bentley *et al.*, 1988). When speract binds to the receptor, it induces cGMP production, which activates a K^+-selective ion channel (Cook and Babcock, 1993), causing a hyperpolarization, as described in the Introduction. This hyperpolarization stimulates Na^+/H^+ exchange and leads to intracellular alkalinization. It was reported that an increase in sperm pHi induces dephosphorylation of GC and decreases its enzymatic activity in *L. pictus* and *Arbacia punctulata* (Bentley *et al.*, 1986; Ward *et al.*, 1986). Considering the effect of pHi on the phosphorylation state of GC, our results suggest that the allosteric interactions between GC and the speract receptor are influenced by pHi. These interactions may also explain why it has been difficult to solubilize the speract receptor with detergent in a functional state (see Fig. 6a). Long-time (30 min) incubation of sperm in NaFSW and DCFSW induced the irreversible inactivation of speract receptor (data not shown). It will be interesting to study which chemical modifications are induced by these treatments on the speract receptor or receptor-associated proteins like GC. Real-time measurements of speract binding to its receptor utilizing the fluorescence quenching method may reveal further details of how the receptor is regulated.

Physiological role of speract. The speract–receptor k_{on} and k_{off} that were determined in this study prompted us to reconsider the physiological role of speract. This peptide has been proposed to attract sperm toward the egg; however, its chemotactic activity has never been demonstrated under physiological conditions. During chemotaxis, a common feature of sperm swimming is a short turn (less than 0.5 s) involving asymmetric flagellar bending, termed chemotactic turning, that changes swimming direction (reviewed in Miller, 1985). Sperm $[Ca^{2+}]$i probably increases when chemotactic turning occurs *in vivo*, since asymmetric flagellar beating can be obtained *in vitro* in demembranated sea urchin sperm at high Ca^{2+} concentrations (Brokaw, 1979). The external Ca^{2+} requirement for chemotaxis supports this idea (Ward *et al.*, 1985). Chemotactic turning occurs when sperm swim away from the source of chemoattractant. Thus, it was proposed that sperm $[Ca^{2+}]$i may increase when chemoattractants dissociate from the receptors (Miller, 1985). This seems unlikely for the speract receptor since the k_{off} obtained in this study is too small. Cook *et al.* (1994) proposed that sperm $[Ca^{2+}]$i is maintained low as long as sperm Em is hyperpolarized by continuous activation of the speract receptor. Thus, when sperm swim toward the egg (positive and steep gradient of speract), $[Ca^{2+}]$i does not increase. Instead, when sperm swim in the wrong direction (insufficiently steep or negative speract gradient), $[Ca^{2+}]$i would increase, triggering chemotactic turning. Therefore, a receptor having a low k_{off} could function in chemotaxis, considering that there are plenty of speract receptors on the sperm plasma membrane (6×10^4/cell). However, when most of the receptors are saturated with speract, sperm $[Ca^{2+}]$i would increase anyhow, changing the swimming direction of sperm before it reaches the egg plasma membrane. Taking into account the k_{on} and k_{off} values from this study and the speract concentration in egg jelly (μM), it can be estimated that 99% of the receptors would be occupied within 0.2 s inside this layer.

Mammalian sperm hyperactivation may offer a clue to solve this paradox (reviewed in Suarez, 1996). In the female reproductive tract, mammalian sperm display asymmetric and high-amplitude flagellar waves accompanied with $[Ca^{2+}]$i elevation (Suarez and Dai, 1995), named hyperactivation. Hyperactivated hamster sperm progress more efficiently in high-viscosity medium than normally activated sperm do, although they show nonprogressive movement in low-viscosity medium (Suarez *et al.*, 1991). Hyperactivation may help mammalian sperm to penetrate the cumulus matrix and the zona pellucida, as was shown in hamster (Stauss *et al.*, 1995). In analogy, speract may induce in sea urchin sperm a hyperactivated-like flagellar movement inside the jelly coat to accelerate sperm penetration through this layer. Sea urchin sperm extrude a short (0.5 μm) acrosomal process upon the acrosome reaction and must keep swimming to reach the egg plasma membrane. Thus, for sea urchin fertilization, sperm penetration through the jelly coat is critical, and speract could play a key role in this process. Therefore, we propose that the speract-induced $[Ca^{2+}]$i increase triggers chemotactic turning in normal seawater (low viscosity), and after sperm reach the egg jelly coat (high viscosity), it accelerates sperm penetration (enhances progressiveness) through this layer. Further experiments will be needed to test this working hypothesis.

ACKNOWLEDGMENTS

We are grateful to Paul Gaytán and Timoteo Olamendi for technical assistance with the HPLC and amino acid analysis, respectively. We thank Dr. M. Yoshida for helpful comments on sperm chemotaxis, Dr. C. Treviño and Dr. I. Weyand for their valuable suggestions regarding the manuscript, and Lucia de De La Torre for determining the speract responses in *L. pictus* sperm. This work was supported by grants from Consejo Nacional de Ciencia y Tecnología, Dirección General de Asuntos del Personal Académico–UNAM, the Howard Hughes Medical Institute, and the International Center for Genetic Engineering and Biotechnology.

REFERENCES

Babcock, D. F., Bosma, M. M., Battaglia, D. E., and Darszon, A. (1992). Early persistent activation of sperm K^+ channels by the egg peptide speract. *Proc. Natl. Acad. Sci. USA* **89,** 6001–6005.

Beltrán, C., Zapata, O., and Darszon, A. (1996). Membrane potential regulates sea urchin sperm adenylylcyclase. *Biochemistry* **35,** 7591–7598.

Bentley, J. K., Tubb, D. J., and Garbers, D. L. (1986). Receptor-mediated activation of spermatozoan guanylate cyclase. *J. Biol. Chem.* **261,** 14859–14862.

Bentley, J. K., Khatra, A. S., and Garbers, D. L. (1988). Receptor-mediated activation of detergent-solubilized guanylate cyclase. *Biol. Reprod.* **39,** 639–647.

Brokaw, C. J. (1979). Calcium-induced asymmetrical beating of Triton-demembranated sea urchin sperm flagella. *J. Cell Biol.* **82,** 401–411.

Cardullo, R. A., Herrick, S. B., Peterson, M. J., and Dangott, L. J. (1994). Speract receptors are localized on sea urchin sperm flagella using a fluorescent peptide analog. *Dev. Biol.* **162,** 600–607.

Cook, S. P., and Babcock, D. F. (1993). Selective modulation by cGMP of the K^+ channel activated by speract. *J. Biol. Chem.* **268,** 22402–22407.

Cook, S. P., Brokaw, C. J., Muller, C. H., and Babcock, D. F. (1994). Sperm chemotaxis: Egg peptides control cytosolic calcium to regulate flagellar responses. *Dev. Biol.* **165,** 10–19.

Dangott, L. J., and Garbers, D. L. (1984). Identification and partial characterization of the receptor for speract. *J. Biol. Chem.* **259,** 13712–13716.

Darszon, A., Labarca, P., Nishigaki, T., and Espinosa, F. (1999). Ion channels in sperm physiology. *Physiol. Rev.* **79,** 481–510.

Galindo, B. E., Beltrán, C., Cragoe, E. J., Jr., and Darszon, A. (2000). Participation of a K^+ channel modulated directly by cGMP in the speract-induced signaling cascade of *Strongylocentrotus purpuratus* sea urchin sperm. *Dev. Biol.* **221,** 285–294.

Garbers, D. L., Watkins, H. D., Hansbrough, J. R., Smith, A., and Misono, K. S. (1982). The amino acid sequence and chemical synthesis of speract and of speract analogues. *J. Biol. Chem.* **257,** 2734–2737.

Gauss, R., Seifert, R., and Kaupp, U. B. (1998). Molecular identification of a hyperpolarization-activated channel in sea urchin sperm. *Nature* **393,** 583–587.

González-Martínez, M. T., Guerrero, A., Morales, E., de De La Torre, L., and Darszon, A. (1992). A depolarization can trigger Ca^{2+} uptake and the acrosome reaction when preceded by a hyperpolarization in *L. pictus* sea urchin sperm. *Dev. Biol.* **150,** 193–202.

Harumi, T., Hoshino, K., and Suzuki, N. (1992). Effects of sperm-activating peptide I on *Hemicentrotus pulcherrimus* spermatozoa in high potassium sea water. *Dev. Growth Differ.* **34,** 163–172.

Hulme, E. C., and Birdsall, N. J. M. (1992). Strategy and tactics in receptor-binding studies. *In* "Receptor–Ligand Interactions" (E. C. Hulme, Ed.), pp. 63–176. Oxford Univ. Press, New York.

Labarca, P., Santi, C., Zapata, O., Morales, E., Beltrán, C., Liévano, A., and Darszon, A. (1996). A cAMP regulated K^+-selective channel from the sea urchin sperm plasma membrane. *Dev. Biol.* **174,** 271–280.

Lee, H. C., and Garbers, D. L. (1986). Modulation of the voltage-sensitive Na^+/H^+ exchange in sea urchin spermatozoa through membrane potential changes induced by the egg peptide speract. *J. Biol. Chem.* **261,** 16026–16032.

Miller, R. L. (1985). Sperm chemo-orientation in the metazoa. *In* "Biology of Fertilization" (C. B. Metz and A. Monroy, Eds.), Vol. 2, pp. 275–337. Academic Press, New York.

Nishigaki, T., Chiba, K., Miki, W., and Hoshi, M. (1996). Structure and function of asterosaps, sperm-activating peptides from the jelly coat of starfish eggs. *Zygote* **4,** 237–245.

Nishigaki, T., Chiba, K., and Hoshi, M. (2000). A 130-kDa membrane protein of sperm flagella is the receptor for asterosaps, sperm-activating peptides of starfish *Asterias amurensis*. *Dev. Biol.* **219,** 154–162.

Roos, A., and Boron, W. F. (1981). Intracellular pH. *Physiol. Rev.* **61,** 296–434.

Schackmann, R. W., and Chock, P. B. (1986). Alteration of intracellular [Ca^{2+}] in sea urchin sperm by the egg peptide speract. Evidence that increased intracellular Ca^{2+} is coupled to Na^+ entry and increased intracellular pH. *J. Biol. Chem.* **261,** 8719–8728.

Shimizu, T., Yoshino, K., and Suzuki, N. (1994). Identification and characterization of putative receptors for sperm-activating peptide I (SAP-I) in spermatozoa of sea urchin *Hemicentrotus pulcherrimus*. *Dev. Growth Differ.* **36,** 209–221.

Smith, A. C., and Garbers, D. L. (1983). The binding of an ^{125}I-speract analogue to spermatozoa. *In* "Biochemistry of Metabolic Processes" (D. L. F. Lennon, F. W. Stratman, and R. N. Zahlten, Eds.), pp. 15–28. Elsevier, New York.

Stauss, C. R., Votta, T. J., and Suarez, S. S. (1995). Sperm motility hyperactivation facilitates penetration of the hamster zona pellucida. *Biol. Reprod.* **53,** 1280–1285.

Suarez, S. S. (1996). Hyperactivated motility in sperm. *J. Androl.* **17,** 331–335.

Suarez, S. S., and Dai, X. (1995). Intracellular calcium reaches different levels of elevation in hyperactivated and acrosome-reacted hamster sperm. *Mol. Reprod. Dev.* **42,** 325–333.

Suarez, S. S., Katz, D. F., Owen, D. H., Andrew, J. B., and Powell, R. L. (1991). Evidence for the function of hyperactivated motility in sperm. *Biol. Reprod.* **44,** 375–381.

Suzuki, N. (1995). Structure, function and biosynthesis of sperm-activating peptides and fucose sulfate glycoconjugate in the extracellular coat of sea urchin eggs. *Zool. Sci.* **12,** 13–27.

Suzuki, N., Nomura, K., Ohtake, H., and Isaka, S. (1981). Purification and the primary structure of sperm-activity peptides from the jelly coat of sea urchin eggs. *Biochem. Biophys. Res. Commun.* **99,** 1238–1244.

Suzuki, N., and Garbers, D. L. (1984). Stimulation of sperm respiration rates by speract and resact at alkaline extracellular pH. *Biol. Reprod.* **30,** 1167–1174.

Ward, G. E., Brokaw, C. J., Garbers, D. L., and Vacquier, V. D. (1985). Chemotaxis of *Arbacia punctulata* spermatozoa to resact, a peptide from the egg jelly layer. *J. Cell Biol.* **101,** 2324–2329.

Ward, G. E., Moy, G. W., and Vacquier, V. D. (1986). Phosphorylation of membrane-bound guanylate cyclase of sea urchin spermatozoa. *J. Cell Biol.* **103,** 95–101.

Yamaguchi, M., Niwa, T., Kurita, M., and Suzuki, N. (1987). The participation of speract in the acrosome reaction of *Hemicentrotus pulcherrimus*. *Dev. Growth Differ.* **30,** 159–167.

Yoshino, K., and Suzuki, N. (1992). Two classes of receptor specific for sperm-activating peptide III in sand-dollar spermatozoa. *Eur. J. Biochem.* **206,** 887–893.

Received for publication October 21, 1999
Revised February 10, 2000
Accepted April 5, 2000